



Deposited via The University of Sheffield.

White Rose Research Online URL for this paper:

<https://eprints.whiterose.ac.uk/id/eprint/89241/>

Version: Accepted Version

---

**Article:**

Bellasio, C. and Griffiths, H. (2013) Acclimation to low light by C4 maize: implications for bundle sheath leakiness. *Plant, Cell and Environment*, 37 (5). 1046 - 1058. ISSN: 0140-7791

<https://doi.org/10.1111/pce.12194>

---

**Reuse**

Items deposited in White Rose Research Online are protected by copyright, with all rights reserved unless indicated otherwise. They may be downloaded and/or printed for private study, or other acts as permitted by national copyright laws. The publisher or other rights holders may allow further reproduction and re-use of the full text version. This is indicated by the licence information on the White Rose Research Online record for the item.

**Takedown**

If you consider content in White Rose Research Online to be in breach of UK law, please notify us by emailing [eprints@whiterose.ac.uk](mailto:eprints@whiterose.ac.uk) including the URL of the record and the reason for the withdrawal request.

# Acclimation to Low Light by C4 maize: Implications for Bundle Sheath Leakiness

Chandra Bellasio and Howard Griffiths

Physiological Ecology Group, Department of Plant Sciences, University of Cambridge, Downing Street, Cambridge, CB2 3EA, UK;

Correspondence: C. Bellasio; E-Mail: chandra.bellasio@plantsci.cam.ac.uk

## Abstract

C4 plants have a biochemical carbon concentrating mechanism (CCM) that increases CO<sub>2</sub> concentration around Rubisco in the bundle sheath (BS). Under limiting light, the activity of the CCM generally decreases, causing an increase in leakiness, ( $\Phi$ ), the ratio of CO<sub>2</sub> retrodiffusing from the BS relative to C4 carboxylation processes. Maize plants were grown under high and low light regimes (respectively HL, 600 vs LL, 100  $\mu\text{E m}^{-2} \text{s}^{-1}$ ). Short term acclimation of  $\Phi$  was compared from isotopic discrimination ( $\Delta$ ), gas exchange and photochemistry. Direct measurement of respiration in the light, and ATP production rate ( $J_{ATP}$ ), allowed us use a novel approach to derive  $\Phi$ , compared to the conventional fitting of measured and predicted  $\Delta$ . HL grown plants responded to decreasing light intensities with the well-documented increase in  $\Phi$ . Conversely, LL plants showed a constant  $\Phi$  which has not been observed previously. We explain the pattern by two contrasting acclimation strategies: HL plants maintained a high CCM activity at LL, resulting in high CO<sub>2</sub> overcycling and increased  $\Phi$ ; LL plants acclimated by downregulating the CCM, effectively optimising scarce ATP supply. This surprising plasticity may limit the impact of  $\Phi$ -dependent carbon losses in leaves becoming shaded within developing canopies.

## Keywords

Carbon isotope discrimination; C4 photosynthesis;  $\Delta^{13}\text{C}$ ; *Zea mays L*; efficiency; bundle sheath conductance;  $g_{BS}$ .

## Introduction

The C4 metabolic syndrome evolved from C3 photosynthesis under declining ambient CO<sub>2</sub> and increasing transpiration demand in semi-arid environments (Griffiths *et al.*, 2013, Osborne & Sack, 2012). In these environments, characterized by high irradiances (where energy supply is not limiting) and high temperatures, C4 plants have higher photosynthetic rates than C3 plants

25 (Percy & Ehleringer, 1984). For this reason many C4 plants are important agricultural crops and  
26 weeds: maize, for example, has been the world's leading grain production cereal (FAO, 2012).  
27 Following concerns about climate change, the high productivity of C4 plants in warm climates  
28 has drawn additional attention to C4 physiology, also with the goal of introducing 'beneficial'  
29 C4 traits into C3 crops such as rice (Covshoff & Hibberd, 2012, Kajala *et al.*, 2011, Sheehy,  
30 2008).

31 The high productivity of C4 plants derives from an active suppression of the oxygenase  
32 activity of Rubisco by means of a biochemical carbon concentrating mechanism (CCM) that  
33 concentrates CO<sub>2</sub> in the cellular compartment where Rubisco is exclusively expressed (bundle  
34 sheath, BS). The CCM has a notable metabolic cost (a theoretical minimum of 2 moles of ATP  
35 per mole of CO<sub>2</sub> assimilated) (Furbank *et al.*, 1990) and involves complex anatomical and  
36 biochemical machinery that decrease efficiency when light is limiting.

37 Although up to 50 % of C4 crop canopy photosynthesis may be carried out by shaded leaves  
38 (Baker & Long, 1988), light limitations play an important role in limiting canopy productivity,  
39 and severe effects on net canopy photosynthetic uptake have been reported (Kromdijk *et al.*,  
40 2008). Most leaves progressively acclimate to shade, since they emerge at the top of the canopy  
41 (as high light leaves) and become shaded by newly emerging leaves. This permanent long-term  
42 acclimation is accompanied by a transitory short-term acclimation response (e.g. daily shading).  
43 Understanding acclimation strategies, i.e. how C4 metabolism copes with light limitations, is  
44 therefore relevant to crop production as well as providing insights for C4 energetic efficiency.

45 This paper investigates the influence of long-term acclimation on C4 inefficiencies under low  
46 light intensities. Previous studies have associated the inefficiency of the CCM under low light to  
47 an increase in leakiness ( $\Phi$ ), i.e. the rate of CO<sub>2</sub> retrodiffusion out of the BS relative to the rate of  
48 PEP carboxylation ( $V_P$ ) [for review (Ubierna *et al.*, 2011)].  $\Phi$  is inevitable and an inherent  
49 feature of a biochemical CCM because a CO<sub>2</sub> concentration gradient is established by  
50 overcycling CO<sub>2</sub> between cellular compartments connected by plasmodesmata.  $\Phi$  is considered a  
51 wasteful process since the refixation of that escaping CO<sub>2</sub> results in an additional ATP cost of the  
52 CCM [ $\Phi$  times higher than the theoretical minimum of 2 ATP per CO<sub>2</sub> (Furbank *et al.*, 1990,  
53 Tazoe *et al.*, 2008)].  $\Phi$  results in enriched <sup>13</sup>CO<sub>2</sub> retrodiffusing from BS, thus enabling  $\Phi$  to be  
54 estimated by studying real-time carbon isotope discrimination during photosynthesis, as  $\Delta_{OBS}$   
55 (Evans *et al.*, 1986).

56  $\Phi$  is one of the discrimination processes operating in C4 photosynthesis that were resolved  
57 into weighted individual fractionations by the model originally derived by G.D. Farquhar (1983).  
58 In the model, diffusion in air, dissolution in water, PEP carboxylation, mitochondrial  
59 decarboxylation, Rubisco carboxylation and diffusion through plasmodesmata are assigned  
60 individual fractionation values. The magnitude of the component fractionation effects are  
61 weighted by the gradient in CO<sub>2</sub> concentrations between the different cellular compartments. The  
62 estimation of these concentrations is not entirely straightforward.  $C_a$ , the atmospheric CO<sub>2</sub>

63 concentration in the cuvette, can be measured directly with the gas exchange analyser.  $C_i$ , the  
64  $\text{CO}_2$  concentration in the substomatal cavity, and  $C_M$ , the  $\text{CO}_2$  concentration in mesophyll cells,  
65 are calculated using the equations for steady-state photosynthesis (Farquhar *et al.*, 1980, von  
66 Caemmerer & Farquhar, 1981).  $C_{BS}$ , the  $\text{CO}_2$  concentration in BS, cannot be measured directly  
67 and is either assumed or estimated. When a large  $C_{BS}$  is assumed [e.g. (Kromdijk *et al.*, 2008,  
68 Pengelly *et al.*, 2010, Tazoe *et al.*, 2008)] an evident bias is introduced for high leakiness values  
69 (Ubierna *et al.*, 2011). When  $C_{BS}$  is estimated through a model for  $\text{C}_4$  photosynthesis (von  
70 Caemmerer, 2000), a parameterization with assimilation ( $A$ ), total ATP production rate ( $J_{ATP}$ ),  
71 respiration in the light ( $R_{LIGHT}$ ) and bundle sheath conductance ( $g_{BS}$ ) is needed.

72 Measurement of  $A$ ,  $J_{ATP}$  and  $R_{LIGHT}$  present some technical issues. Assimilation can be  
73 measured directly: good practices allowing measurements with suitable accuracy are well  
74 codified from studies on  $\text{C}_3$  plants (Flexas *et al.*, 2007, Long & Bernacchi, 2003, Pons *et al.*,  
75 2009).  $J_{ATP}$ ,  $R_{LIGHT}$  and  $g_{BS}$  are more difficult to distinguish experimentally and the approach  
76 followed by the latest studies leaves room for improvement: i)  $J_{ATP}$  has been traditionally  
77 resolved from a theoretical relationship between quantum yield of photosystem II and ATP  
78 production rate. This estimate relies on parameters that are difficult to measure, some of which  
79 are still unknown (von Caemmerer, 2000). ii)  $R_{LIGHT}$  has often been assumed equal to respiration  
80 in the dark, which is relatively simple to measure [e.g. (Ubierna *et al.*, 2013)]. Growing  
81 awareness of the mechanisms of regulation of respiration in the light (Tcherkez *et al.*, 2008)  
82 reveal the limits of the traditional assumption. iii)  $g_{BS}$  has been traditionally resolved by  
83 calculating a ‘modelled’ isotopic discrimination during photosynthesis,  $\Delta_{MOD}$ , and fitting  $\Delta_{MOD}$  to  
84 the observed discrimination during photosynthesis  $\Delta_{OBS}$  (later referred to as  $\Delta / \Delta$  approach) [for  
85 review (Ubierna *et al.*, 2011)]. This approach introduces a certain degree of circularity, since  $C_{BS}$   
86 and  $\Phi$  are both estimated from  $\Delta_{OBS}$ .

87 In order to develop these technical issues we introduced three major experimental advances: i)  
88  $R_{LIGHT}$  was measured through the combined use of fluorescence and gas exchange (Yin *et al.*,  
89 2011a); ii) the total ATP production rate,  $J_{ATP}$ , was measured at low  $\text{O}_2$  and the value was  
90 corrected by the small ATP demand for photorespiration (Yin & Struik, 2009, Yin *et al.*, 2011b);  
91 iii) using the precise estimate of  $J_{ATP}$ ,  $g_{BS}$  could be estimated by curve fitting based on  $J_{ATP}$  ( $J / J$   
92 approach). Since  $g_{BS}$  and  $\Phi$  were derived from independent datasets, the  $J / J$  approach did not  
93 suffer the circularity of the  $\Delta / \Delta$  approach; finally, plants were grown under two contrasting  
94 light regimes with the lowest ( $100 \mu\text{E m}^{-2} \text{s}^{-1}$ ) well below that used in comparable studies  
95 (Kromdijk *et al.*, 2010, Pengelly *et al.*, 2010, Tazoe *et al.*, 2008).

96 Results showed that long-term acclimation influenced the way maize plants responded to  
97 decreasing light intensities. When plants grown in high light (HL,  $600 \mu\text{E m}^{-2} \text{s}^{-1}$ ) were exposed  
98 to decreasing light intensities, they responded with an increase in  $\Phi$ . Conversely and in contrast  
99 to the pattern reported in previous studies, plants grown in low light (LL) did not show any  
100 increase in  $\Phi$ . By refitting the  $\text{C}_4$  model we hypothesized the possible underlying physiological

101 processes. HL and LL plants deployed a contrasting strategy at limiting light intensities: while  
102 HL plants maintained a high CCM activity, resulting in high CO<sub>2</sub> overcycling, LL plants  
103 decreased the CCM activity and coped with the resulting decrease of CO<sub>2</sub> flow to BS by  
104 adjusting carboxylase activity or bundle sheath conductance, effectively optimising scarce ATP  
105 supply.

## 106 **Materials and Methods**

### 107 *Plants*

108 Maize plants were grown at the Plant Growth Facility located at the University of Cambridge  
109 Botanic Garden in controlled environment growth rooms (Conviron Ltd, Winnipeg, Canada) set  
110 at 16 h day length, temperature of 25 °C / 23 °C (day / night) and 40 % relative humidity.

111 The growth protocol was designed to standardize age and watering conditions throughout the  
112 experiment. Every Monday, seeds of *Zea mays* L. (F1 Hybrid PR31N27, Pioneer Hi-bred,  
113 Cremona, Italy) were sown in 1.5 L pots filled with Levington pro M3 pot & bedding compost  
114 (Scotts Miracle-Gro, Godalming, UK) and positioned in HL (PAR = 600 μE m<sup>-2</sup> s<sup>-1</sup>) or in LL  
115 (PAR = 100 μE m<sup>-2</sup> s<sup>-1</sup>). LL intensity was obtained through shading to mimic the understory of a  
116 canopy. Plants were manually watered daily with particular care to avoid overwatering. At the  
117 fully expanded 4<sup>th</sup> leaf stage (3 weeks, HL; 4 weeks, LL) plants were measured once and then  
118 discarded.

### 119 *Gas exchange measurements with concurrent PSI / PSII Yield and carbon isotopic* 120 *discrimination*

121 The experimental setup for measuring  $J_{ATP}$  and  $\Delta$  concurrently on the same sample consisted  
122 of an infra-red gas analyzer (IRGA), a Dual PAM and a trapping line. The IRGA, a LI6400XT  
123 (Li-Cor, Lincoln Nebraska, USA), was fitted with a 6400-06 PAM2000 adapter, holding a fiber  
124 probe in the upper leaf cuvette distant enough to avoid shading. Light was provided by a Li-Cor  
125 6400-18 RGB light source, positioned to uniformly illuminate the leaf. Measurements with low  
126 gas flow, indispensable to measure discrimination at low light intensities, required careful  
127 optimization to minimize leaks. Neoprene gaskets were used on both sides of the cuvette and a  
128 tiny ridge of vacuum grease was laid on gaskets so as to seal the leaf upon closure. A 2 % O<sub>2</sub> /  
129 N<sub>2</sub> (pre-mixed, BOC, UK) or ambient air was CO<sub>2</sub>-scrubbed with soda lime and humidified to a  
130 dew point of 19 °C upstream of the inlet. Natural abundance CO<sub>2</sub> ( $\delta = -9.46$  ‰) used to reduce  
131 artefacts (Gandin & Cousins, 2012, Ubierna *et al.*, 2011) was added from a cylinder (Isi, Wien,  
132 A), with use of the CO<sub>2</sub> injection unit of the IRGA.

133 To determine the most suitable 'high CO<sub>2</sub>' concentration (used to measure  $J_{ATP}$ , see below) a  
134 set of pilot light response curves at decreasing  $C_a$  were performed. 600 μmol mol<sup>-1</sup> was chosen

135 because i) further increases in CO<sub>2</sub> concentration did not result in higher A; ii) stomatal closure  
136 was not strongly induced; iii) it was sufficiently similar to lab CO<sub>2</sub> concentration (550 μmol mol<sup>-1</sup>)  
137 to minimize the problem of CO<sub>2</sub> diffusion out of the cuvette (Flexas *et al.*, 2007). Gas flow  
138 was set at 150 μmol s<sup>-1</sup> (PAR = 500 and 250 μE m<sup>-2</sup> s<sup>-1</sup>), 100 μmol s<sup>-1</sup> (PAR = 125 μE m<sup>-2</sup> s<sup>-1</sup>), 75  
139 μE s<sup>-1</sup> (PAR = 75 μE m<sup>-2</sup> s<sup>-1</sup>) and 50 μmol s<sup>-1</sup> (PAR ≤ 50 μE m<sup>-2</sup> s<sup>-1</sup>). Block temperature was  
140 controlled at 26 °C. Stomatal ratio was set to 0.7 (Driscoll *et al.*, 2006). Water pressure deficit  
141 was carefully kept below 1 KPa to foster stomatal opening. PSI and PSII yield were measured in  
142 reflectance mode with a Dual Pam-F (Heinz Walz GmbH, Effeltrich, D). Pulse intensity was set  
143 to 20 mE m<sup>-2</sup> s<sup>-1</sup>, enough to saturate *F* and *P* signals (which occurred between 8 and 10 mE m<sup>-2</sup> s<sup>-1</sup>  
144 <sup>1</sup>, data not shown). To measure Δ<sub>OBS</sub>, the IRGA was connected to a cryogenic H<sub>2</sub>O and CO<sub>2</sub>  
145 trapping-purification line (Griffiths *et al.*, 1990), that concentrated the CO<sub>2</sub> in the low IRGA  
146 flow rates. The trapping line consisted of a glass coil in which CO<sub>2</sub> and water were frozen under  
147 liquid N<sub>2</sub>. 40-50 μmol s<sup>-1</sup> of gas, taken either from the leaf cuvette or from the reference gas tube,  
148 were trapped for 15 min. A minimum surplus was vented to ensure overpressure in the piping.  
149 To match IRGAs the sample flow was periodical redirected towards the IRGA reference channel.  
150 After trapping, CO<sub>2</sub> was purified by differential sublimation in a sealed vial for mass  
151 spectrometry.

152 Measurements were performed with a rigid acclimation routine. Before measurements plants  
153 were dark-adapted and watered to pot capacity. The distal part of the youngest fully expanded  
154 leaf was clamped in the leaf cuvette in the dark. Maximum yield of PSII (*F<sub>v</sub>* / *F<sub>m</sub>*) and *P<sub>m</sub>*, signal  
155 were registered (details of PSI measurements are reported in supporting Figure S 2). An initial  
156 light response curve (500, 250, 125, 75, 50 and 30) μE m<sup>-2</sup> s<sup>-1</sup> was registered at 2 % O<sub>2</sub> and *C<sub>a</sub>* =  
157 600 μmol / mol. Leaves were acclimated for > 30 min at the beginning and > 15 min between  
158 each change in PAR level. At steady state, a saturating pulse was applied and assimilation was  
159 recorded every 30 s for 5 min. A second light response curve was registered at 21 % O<sub>2</sub> and  
160 reference CO<sub>2</sub> set at 400 μmol / mol, during which exhaust gas was trapped to determine Δ<sub>OBS</sub>. A  
161 rigorous routine, consisting of 20 min acclimation, 15 min trapping, 7 min acclimation and 15  
162 min trapping was followed for each PAR level. Assimilation was recorded every 30 s throughout  
163 trapping, while pulses were applied twice to minimise photobleaching.

164 This routine yielded a total of 12 CO<sub>2</sub> samples collected during trapping and 6 reference gas  
165 collected during acclimation for each of 4 LL plants and 3 HL plants. CO<sub>2</sub> was analysed directly  
166 with a VG SIRA dual inlet isotope ratio mass spectrometer (modified and maintained by Pro-Vac  
167 Services Ltd, Crewe, UK). Values were corrected for presence of N<sub>2</sub>O and <sup>17</sup>O. Δ<sub>OBS</sub> was  
168 calculated according to Evans *et al.* (1986) and reflects an average for 15 minutes continuous  
169 photosynthetic discrimination (equations are reported in supporting Text 2).

170 *Respiration in the light R<sub>LIGHT</sub>*

171 Respiration in the light was estimated independently at 2 % O<sub>2</sub> and at 21 % O<sub>2</sub> with the  
 172 chlorophyll fluorescence method proposed by Yin and colleagues (Yin & Struik, 2009, Yin *et*  
 173 *al.*, 2011a). Briefly, *A* was plotted against PAR · *Y(II)* / 3 (where *Y(II)* is PSII yield, Eqn 12, Supp.  
 174 information, the coefficient 3 was maintained to ease comparison with previous work); the y-  
 175 intercept of the linear regression gives an estimation of  $-R_{LIGHT}$  (Supporting Fig. 1).

176 *Total ATP production rate J<sub>ATP</sub>*

177 *J<sub>ATP</sub>* was derived from gas exchanges at low O<sub>2</sub> concentration and corrected under ambient O<sub>2</sub>.  
 178 We adopted a gas exchange / fluorescence approach as it did not rely on assumptions or  
 179 uncertain parameterization. This method was used in previous studies (Yin & Struik, 2009, Yin  
 180 *et al.*, 2011b) where a linear relationship between *J<sub>ATP</sub>* and electron transport rate, ETR (Krall &  
 181 Edwards, 1990, Oberhuber *et al.*, 1993) was assumed. We observed a slight deviation of *J<sub>ATP</sub>* /  
 182 ETR from linearity at irradiance 500 μE m<sup>-2</sup> s<sup>-1</sup>, consistent with previous data (D'Ambrosio *et al.*,  
 183 2003). Instead of linearizing the relationship, we scaled *J<sub>ATP</sub>* to ETR individually at each  
 184 irradiance (the calculation is identical to the original method when the relationship is linear).

185 *J<sub>ATP Low O<sub>2</sub></sub>* was calculated from gross assimilation (*GA*) measured under low O<sub>2</sub>. Under low  
 186 O<sub>2</sub>,  $\Phi$  and photorespiration are minimal (Kromdijk *et al.*, 2010) and the ATP requirement of *GA*  
 187 (3 / 0.59) is similar to the theoretical minimum (Yin & Struik, 2009, Yin *et al.*, 2011b).  
 188

$$J_{ATP Low O_2} = \frac{3 GA_{Low O_2}}{0.59} \quad (1)$$

189  
 190 *J<sub>ATP</sub>* (at ambient O<sub>2</sub>) was calculated from *J<sub>ATP Low O<sub>2</sub></sub>* by correcting for photorespiration using  
 191 ETR as a scaling factor.

$$J_{ATP} = \frac{J_{ATP Low O_2} Y(II)}{Y(II)_{Low O_2}} \quad (2)$$

193  
 194 Eqn 2 was calculated at each light intensity, the results are the symbols shown in figure 3 A.  
 195 Note that, of the components of ETR, only *Y(II)* shows in Eqn 2 as PAR and compound  
 196 conversion efficiency (*s'*) simplify. For the derivation of Eqn 2 see supporting Text 1. In C4  
 197 plants photorespiration is low, therefore the difference between *J<sub>ATP Low O<sub>2</sub></sub>* and *J<sub>ATP</sub>* was minimal  
 198 (c. 1 %). Photochemical yield appears both at the numerator and at the denominator of Eqn 2,  
 199 therefore this robust approach is independent of systematic errors that affect both *Y(II)* and  
 200 *Y(II)<sub>Low O<sub>2</sub></sub>*.

201 This procedure to derive  $J_{ATP}$  was particularly suitable to parameterize and fit the C4 model.  
 202 Since  $J_{ATP}$  was measured concurrently to gas exchange and isotopic discrimination, it represented  
 203 the actual  $J_{ATP}$  of the portion of the leaf that was subject to isotopic discrimination  
 204 measurements. Furthermore,  $J_{ATP}$  was derived under the same assumptions of the C4 model (Eqn  
 205 4 to 10, see below). Under these assumptions  $J_{ATP}$  represented the fraction of ATP available for  
 206 photosynthesis and it was not influenced by the ATP allocation to alternative sinks.

### 207 *Estimated leakiness from isotopic discrimination*

208 Leakiness was resolved from carbon isotope discrimination (Farquhar, 1983, Farquhar &  
 209 Cernusak, 2012, Ubierna *et al.*, 2013):

210

$$\Phi_{id} = \frac{C_{BS} - C_M}{C_M} \frac{b_4 C_M (1 + t) + a(C_a - C_i) - C_a \Delta_{OBS} (1 - t)}{(1 + t)[C_a \Delta_{OBS} (1 - t) - a(C_a - C_i) - b_3 C_{BS} + s(C_{BS} - C_M)]} \quad (3)$$

211

212 Where the subscript 'id' reminds that  $\Phi$  was obtained from isotopic discrimination,  $C_a$ ,  $C_i$ ,  
 213  $C_{BS}$ ,  $C_M$  are the CO<sub>2</sub> concentrations in the different compartments;  $a$  is the fractionation during  
 214 CO<sub>2</sub> diffusion in air;  $s$  is the fractionation during CO<sub>2</sub> leakage;  $b_3$  is the fractionation of Rubisco  
 215 CO<sub>2</sub> fixation, corrected for respiration and photorespiration;  $b_4$  is the combined fractionation of  
 216 CO<sub>2</sub> ↔ HCO<sub>3</sub><sup>-</sup> conversion and PEPC fixation, corrected for mitochondrial respiration in the  
 217 mesophyll;  $t$  represents the ternary effects; other quantities were previously defined (Table 1).

218  $C_a$  is measured directly by the IRGA, whilst the estimations of  $C_i$ ,  $C_M$  and  $C_{BS}$  require  
 219 modelling.

### 220 *Modelled C4 photosynthesis*

221 The C4 model described below estimated the CO<sub>2</sub> concentrations in the different  
 222 compartments ( $C_i$ ,  $C_M$  and  $C_{BS}$ ) that are required to parameterize Eqn 3.  $C_i$  was estimated through  
 223 the equations for steady state photosynthesis (Farquhar *et al.*, 1980, von Caemmerer & Farquhar,  
 224 1981), directly by the IRGA software.  $C_M$  was calculated from the supply function of M as (von  
 225 Caemmerer, 2000):

226

$$C_M = C_i - \frac{A}{g_M} \quad (4)$$

227

228 Where  $g_M$  is the mesophyll conductance to CO<sub>2</sub>.

229  $C_{BS}$  was derived from the supply function of BS:

230

$$C_{BS} = \frac{L}{g_{BS}} + C_M \quad (5)$$

231

232 Where  $g_{BS}$  is BS conductance to  $CO_2$  and  $L$ , the leakage rate was calculated from M mass  
233 balance:

234

$$L = V_P - R_M - A \quad (6)$$

235

236 Where  $RM$ , M respiration rate in the light was assumed half the  $R_{LIGHT}$ .  $V_P$ , the PEP  
237 carboxylation rate is limited by PEP regeneration and ATP supply. It was calculated by  
238 partitioning  $J_{ATP}$  between C4 activity ( $V_P$ ) and C3 activity (reductive pentose phosphate pathway  
239 + photorespiratory cycle) by means of a partitioning factor ( $x$ , Table 1):

240

$$V_P = \frac{x J_{ATP}}{2} \quad (7)$$

241

242 Eqn 5, 6 and 7 can be combined to give:

243

$$C_{BS} = \frac{\frac{x J_{ATP}}{2} - \frac{R_{LIGHT}}{2} - A}{g_{BS}} + C_M \quad (8)$$

244

245 Eqn 8 describes the dependency of  $C_{BS}$  on the measured quantities  $A$ ,  $R_{LIGHT}$  and  $J_{ATP}$ , as a  
246 function of  $g_{BS}$ .  $g_{BS}$  cannot be estimated directly or be derived from previous studies (it varies  
247 between individuals), so it was estimated by curve fitting. To do so, the C4 model was  
248 rearranged to express a measured quantity.

249 In a first approach (referred to as J / J method) the model was rearranged to express a  
250 modelled ATP production rate  $J_{MOD}$  (Ubierna *et al.*, 2013):

251

$$J_{MOD} = \frac{-y + \sqrt{y^2 - 4wz}}{2w} \quad (9)$$

252

253 Where  $w = \frac{x-x^2}{6A}$ ;  $y = \frac{1-x}{3} \left[ \frac{g_{BS}}{A} + \left( C_M - \frac{R_M}{g_{BS}} - \gamma^* O_M \right) - 1 - \frac{\alpha\gamma^*}{0.047} \right] - \frac{x}{2} \left( 1 + \frac{R_{LIGHT}}{A} \right)$ ;  
 254  $z = \left( 1 + \frac{R_{LIGHT}}{A} \right) \left( R_M - g_{BS} C_M - \frac{7 g_{BS} \gamma^* O_M}{3} \right) + (R_{LIGHT} + A) \left( 1 - \frac{7\alpha\gamma^*}{3 \cdot 0.047} \right)$ ;  $\alpha$  is the fraction of  
 255 PSII activity in BS cells;  $\gamma^*$  is a parameter related to Rubisco  $O_2 / CO_2$  specificity;  $O_M$  is the  $O_2$   
 256 concentration in M; other variables were previously defined (Table 1).

257  $J_{MOD}$  was iteratively calculated at varying  $g_{BS}$  until the  $J_{MOD}$  matched  $J_{ATP}$ . The  $g_{BS}$  value that  
 258 yielded the best fit was assumed as  $g_{BS}$  of that individual plant. This operation can be visualized  
 259 in Figure 3 A: the solid lines represent Eqn 9 calculated for HL (thick solid line) and LL (thin  
 260 solid line), with  $g_{BS}$  varied until the modelled values (solid lines in Figure 3A) matched  $J_{ATP}$   
 261 (symbols in Figure 3 A). Notably, with the J / J approach  $g_{BS}$  was obtained independently of  $\Delta_{OBS}$   
 262 (see discussion).

263 A different approach (referred to as  $\Delta / \Delta$  method) involved rearranging the C4 model to  
 264 express a modelled isotopic discrimination (Kromdijk *et al.*, 2010):  
 265

$$\Delta_{MOD} = a \frac{(C_a - C_i)}{C_a} + (e_s + a_d) \frac{(C_i - C_M)}{C_a} + \frac{b_4 V_P + b_3 L \frac{C_{BS}}{C_{BS} - C_M} - sL}{V_P + L \frac{C_M}{C_{BS} - C_M}} \frac{C_M}{C_a} \quad (10)$$

266  
 267 Where  $(a, a_d, b_3, b_4, e_s, s)$  are the individual contribution to discrimination and other variables  
 268 were previously defined (Table 1).

269  $\Delta_{MOD}$  was iteratively calculated at different  $g_{BS}$ , and the value of  $g_{BS}$  that fitted  $\Delta_{MOD}$  to  $\Delta_{OBS}$   
 270 was assumed as  $g_{BS}$  for that individual. This operation can be visualized in Figure 3 B. The  
 271 dotted lines represent Eqn 10 calculated for HL (thick dotted lines) and LL (thin dotted lines),  
 272 with  $g_{BS}$  varied until  $\Delta_{MOD}$  (dotted lines in Figure 3 B) matched  $\Delta_{OBS}$  (symbols in Figure 3 B).

273 The values obtained for  $C_{BS}$  and  $g_{BS}$ , with the two fitting approaches described, were used to  
 274 derive  $\Phi_{id}$  from isotopic discrimination data  $\Delta_{OBS}$  as described above.

275 Modelled leakiness was calculated to compare results of different modelling approaches:  
 276

$$\Phi_{MOD} = \frac{L}{V_P} \quad (11)$$

277

## 278 Results

279 Maize plants were grown under two different light regimes and their photosynthetic response  
 280 was studied under decreasing light intensities. Carbon isotope discrimination, PSI / PSII  
 281 photochemistry and gas exchange were measured concurrently.  $CO_2$  concentration in BS ( $C_{BS}$ )

282 and bundle sheath conductance ( $g_{BS}$ ) were estimated by implementing a C4 photosynthesis  
283 model. The C4 model was constrained with two different datasets: the ATP production rate  $J_{ATP}$   
284 ( $J/J$  approach) and the real-time isotope discrimination data  $\Delta_{OBS}$  ( $\Delta/\Delta$  approach). In this way  
285 two different sets of values for  $C_{BS}$  and  $g_{BS}$  were estimated and were used, in turn, to resolve  
286 leakiness ( $\Phi_{id}$ ) from  $\Delta_{OBS}$  by Eqn 3.

### 287 *Physiological response to decreasing light intensities*

288 Assimilation ( $A$ ) differentiated LL plant and HL plant responses (Figure 1 A). LL plants had  
289 lower  $A$  at high PAR, but relatively higher  $A$  at lower PAR. Consistently, the compensation point  
290 ( $I$ ) and respiration in the light ( $R_{LIGHT}$ ) of LL plants were lower (Table 2). When low  $O_2$  was  
291 supplied,  $A$  of LL plants increased on average by  $0.3 \mu\text{mol m}^{-2} \text{s}^{-1}$ , while  $A$  of HL plants  
292 increased by an average of  $0.2 \mu\text{mol m}^{-2} \text{s}^{-1}$ .

293 Figure 1 B shows that  $C_i/C_a$  was higher than 0.6 at  $\text{PAR} < 125 \mu\text{E m}^{-2} \text{s}^{-1}$  (LL plants) or  $\text{PAR}$   
294  $< 500 \mu\text{E m}^{-2} \text{s}^{-1}$  (HL plants). This was a remarkable result considering maize typical stomatal  
295 responses e.g. (Ubierna *et al.*, 2013) and reflected efforts made during the measurements to  
296 induce stomatal opening (see methods for details). A high  $C_i/C_a$  was important to maximise the  
297 contribution of biochemical processes to total isotopic discrimination, and it was a prerequisite  
298 for resolution of the isotopic discrimination model. Compared to HL plants, LL plants showed  
299 slightly reduced  $C_i/C_a$ , as a consequence of lower stomatal conductance (Figure 1 C).

300 The photochemical yield of PSII  $Y(II)$  decreased linearly at increasing PAR in both HL plants  
301 (Figure 2 A) and LL plants (Figure 2 B). Consistently, the quantum yield for  $\text{CO}_2$  assimilation  
302 decreased, and a linear relationship between quantum yield of  $\text{CO}_2$  assimilation and  $Y(II)$  was  
303 observed in all samples (Supplementary Figure S 3). In LL plants,  $Y(II)$  was unaffected by  $O_2$   
304 concentration whereas HL plants displayed a tendency to have lower  $Y(II)$  under low  $O_2$  (Figure  
305 2 A). The photochemical yield of PSI  $Y(I)$  decreased at decreasing PAR (Supplementary Figure  
306 S 2). To the best of our knowledge this is the first study where maize  $Y(I)$  is measured together a  
307 complex physiological characterization.

308 The total ATP production rate ( $J_{ATP}$ ) is shown by symbols in Figure 3A.  $J_{ATP}$  was derived  
309 from gross assimilation under low  $O_2$  (Eqn 1) and then corrected for photorespiration at ambient  
310  $O_2$  using the ratio of photochemical yield (Eqn 2). At high PAR,  $J_{ATP}$  of LL plants was lower  
311 than  $J_{ATP}$  of HL plants because of the lower ATP demand for lower  $A$  (Figure 1). At low PAR,  
312  $J_{ATP}$  of LL plants matched  $J_{ATP}$  of HL plants, suggesting that the higher  $A$  of LL plants at limiting  
313 PAR (inset in Figure 1) was achieved through a higher conversion efficiency and lower  
314 respiration rate (Table 2).

315 Isotopic discrimination during photosynthesis ( $\Delta_{OBS}$ ) is shown by symbols in Figure 3 B. In  
316 LL plants  $\Delta_{OBS}$  was relatively low (around 4 ‰) and unaffected by light intensity. In HL plants

317  $\Delta_{OBS}$  increased from 2.6 ‰ at 500  $\mu\text{E m}^{-2} \text{s}^{-1}$  to 22.1 ‰ at 30  $\mu\text{E m}^{-2} \text{s}^{-1}$ . These responses were  
318 confirmed by measurements on an independent batch of plants (Supplementary Figure S 4).

### 319 *Modelled C4 photosynthesis: model fitting and estimation of $g_{BS}$ and $C_{BS}$*

320 An estimate of BS conductance to  $\text{CO}_2$ ,  $g_{BS}$ , was obtained for each individual plant. Table 3  
321 shows that  $g_{BS}$  was lower when obtained through the J / J approach. Table 3 also shows that LL  
322 plants had lower  $g_{BS}$  than HL plants. These  $g_{BS}$  values were used in Eqn 8, the supply function of  
323 BS, to calculate  $C_{BS}$ .  $C_{BS}$  differentiated between fitting approaches. With the J / J approach,  $C_{BS}$   
324 of HL and LL plants were similar, decreasing from (2400 to 1000)  $\mu\text{mol / mol}$  at decreasing  
325 PAR. With the  $\Delta / \Delta$  approach,  $C_{BS}$  was substantially lower than calculated using the J / J  
326 approach and differed between the two growth regimes. In LL plants  $C_{BS}$  ranged from (1700 to  
327 700)  $\mu\text{mol / mol}$ , while in HL plants  $C_{BS}$  ranged from (970 to 570)  $\mu\text{mol / mol}$ .

### 328 *Response of $\Phi_{id}$ to light intensity*

329 Symbols in Figure 4 B and C show that in LL plants leakiness,  $\Phi_{id}$ , derived from real-time  
330 carbon isotope discrimination data,  $\Delta_{OBS}$ , was constant at decreasing PAR, while in HL plants  $\Phi_{id}$   
331 increased hyperbolically at decreasing PAR. To derive  $\Phi_{id}$  from  $\Delta_{OBS}$ , Eqn 3 was parameterized  
332 with the output of the C4 model, fitted with the J / J approach or  $\Delta / \Delta$  approach (compare  
333 symbols in Figure 4 B and C). With the J / J approach (symbols in Figure 4 B), LL plants  $\Phi_{id}$   
334 (triangles) was close to 0.24 and HL plants  $\Phi_{id}$  (squares) ranged from 0.17 to 0.67. With the  $\Delta /$   
335  $\Delta$  approach (Figure 4 C, symbols) LL plants  $\Phi_{id}$  was close to 0.22 (triangles), and HL plants  $\Phi_{id}$   
336 (squares) ranged from 0.16 to 0.49.

### 337 *Modelled leakiness $\Phi_{MOD}$*

338 Figure 4 B shows that with the J / J approach,  $\Phi_{MOD}$  underestimated  $\Phi_{id}$  both in LL and HL  
339 plants. With the  $\Delta / \Delta$  approach (Figure 4 C dotted lines)  $\Phi_{MOD}$  and  $\Phi_{id}$  were not independent  
340 estimates of  $\Phi$  (see discussion).

341 Interestingly, with both approaches  $\Phi_{MOD}$  did not describe the constant  $\Phi_{id}$  observed in LL  
342 plants. In fact, fitting varied  $\Phi_{MOD}$  magnitude, but did not change the shape of the function, with  
343  $\Phi_{MOD}$  hyperbolically increasing at decreasing PAR (compare lines in Figure 4 B and C). As a  
344 consequence, the linear  $\Phi_{id}$  trend observed was not predicted by the conventional fitting but  
345 required a more complex procedure.

### 346 *Model refitting*

347 Figure 5 A shows the values of  $x$  (the ATP partitioning between PEPC activity and C3  
348 activity) that were required to refit  $\Phi_{MOD}$  to  $\Phi_{id}$ . Interestingly,  $x$  showed a contrasting tendency in

349 the two different treatments: in LL plants there was a tendency of fitted  $x$  to decrease at  
350 decreasing light intensities while in HL plants there was no clear trend. Figure 5 B shows the  $g_{BS}$   
351 values that refitted  $\Phi_{MOD}$  to  $\Phi_{id}$ .  $g_{BS}$  differentiated between LL and HL plants: in LL plants there  
352 was a clear decrease of refitted  $g_{BS}$  at decreasing light intensities (Figure 5 B) while in HL plants  
353 refitted  $g_{BS}$  did not show a pattern.

## 354 Discussion

### 355 *Technical optimization: $R_{LIGHT}$ , $J_{ATP}$ and J / J fitting approach*

356 By measuring  $J_{ATP}$  directly, we parameterized the isotopic discrimination model with a  
357 suitable novel approach, independent of  $\Delta_{OBS}$ . Plants were subject to gas exchange and  
358 photochemical investigations at low  $O_2$  and to gas exchange, isotopic discrimination and  
359 photochemical investigation at ambient  $O_2$ . This complex setup allowed estimation of  $R_{LIGHT}$  and  
360 derivation of  $J_{ATP}$  for the portion of the leaf clamped in the cuvette at the very moment that gas  
361 exchange and isotopic discrimination were being measured. The availability of precise  
362 independently estimated values for  $J_{ATP}$ , offered a valid dataset for fitting the C4 model. This ‘J /  
363 J approach’ was used together with isotope discrimination data for the first time in the present  
364 work. In fact in studies where  $J_{ATP}$  was modelled, and therefore not independently obtained, the J  
365 / J fitting was not possible e.g. (Ubierna *et al.*, 2013)]. Nor was it possible when  $J_{ATP}$  was  
366 calculated using parameters derived from leaves differing from those subject to gas exchange,  
367 because, in this case,  $J_{ATP}$  did not strictly represent the portion of the leaf subject to isotopic  
368 discrimination and gas exchange investigations e.g. (Kromdijk *et al.*, 2010).

369 The J / J approach suited the C4 model parameterization. Firstly,  $J_{ATP}$  was derived from gas  
370 exchange measurements under the same assumptions of the C4 model. Under these assumptions  
371  $J_{ATP}$  represented the fraction of ATP available for photosynthesis and was not influenced by the  
372 ATP allocation to alternative sinks. Secondly, the J / J approach did not suffer the circularity of  
373 the  $\Delta / \Delta$  approach, where  $C_{BS}$  and  $g_{BS}$  are not independent, being both derived from  $\Delta_{OBS}$   
374 (Kromdijk *et al.*, 2010, Ubierna *et al.*, 2013). Thirdly, with the J / J approach, the estimate of  $C_{BS}$   
375 and  $g_{BS}$ , relied uniquely on gas exchange and fluorescence data, without requiring isotopic  
376 discrimination data. This had major benefits: i) since there was no amplification of error  
377 dependent on  $\zeta$  (supporting Text 2 and Supporting Table 1),  $J_{ATP}$  could be measured at any light  
378 intensity, even below the compensation point; ii) the equipment was relatively cheap and easy to  
379 maintain; iii) data had low noise / signal ratio.

### 380 *J / J compared to $\Delta / \Delta$*

381 To show these differences and the similarities between the two approaches, model parameters  
382 other than  $g_{BS}$  were kept constant throughout, using consensus values derived from the literature

383 (Table 1). The different approaches yielded different  $g_{BS}$  and  $C_{BS}$  values, but this resulted in  
384 different  $\Phi_{id}$  only in HL plants. Bundle sheath conductance ( $g_{BS}$ ) derived with the J / J approach  
385 was one third of the value of  $g_{BS}$  derived with the  $\Delta / \Delta$  approach. The overall range ( $8.2 \cdot 10^{-4}$  to  
386  $46 \cdot 10^{-4}$ ) mol m<sup>-2</sup> s<sup>-1</sup> was within the range previously reported:  $15 \cdot 10^{-4}$  mol m<sup>-2</sup> s<sup>-1</sup> (Ubierna *et al.*,  
387 2013); ( $8 \cdot 10^{-4}$  to  $103 \cdot 10^{-4}$ ) mol m<sup>-2</sup> s<sup>-1</sup> (Yin *et al.*, 2011b); ( $3.7 \cdot 10^{-4}$  to  $23.5 \cdot 10^{-4}$ ) mol m<sup>-2</sup> s<sup>-1</sup>  
388 (Kromdijk *et al.*, 2010). The corresponding  $C_{BS}$  values estimated with the J / J approach were on  
389 average 70 % higher than those estimated with the  $\Delta / \Delta$  approach. The range we reported (500  
390 to 2500)  $\mu$ mol mol<sup>-1</sup>, was consistent with values reported for maize [for review (von Caemmerer  
391 & Furbank, 2003)]. In spite of these  $C_{BS}$  differences, in LL plants the two approaches yielded  
392 identical  $\Phi_{id}$ , indicating that  $\Phi_{id}$  is fairly insensitive to variations of  $C_{BS}$  when  $\Delta_{OBS}$  is low.  
393 Conversely, in HL plants the two approaches yielded different  $\Phi_{id}$ , because of the big difference  
394 in  $C_{BS}$  and the higher values of  $\Delta_{OBS}$ .

395 Modelled leakiness,  $\Phi_{MOD}$ , is one of the outputs of the C4 model and carries different  
396 information, depending on the C4 model parameterization. With the J / J approach (Figure 4 B  
397 solid lines),  $\Phi_{MOD}$  was calculated with gas exchange and photochemical data only, therefore  
398  $\Phi_{MOD}$  (Figure 4 B lines, Eqn 7) and  $\Phi_{id}$  (Figure 4 B symbols, Eqn 3) represented two  
399 independent estimates of  $\Phi$ . The discrepancy between  $\Phi_{MOD}$  and  $\Phi_{id}$  is dependent on the  
400 different assumptions made in the calculations. One could decrease this discrepancy by  
401 progressively increasing  $g_{BS}$  until the distance between  $\Phi_{MOD}$  and  $\Phi_{id}$  is minimized. Now,  $\Phi_{MOD}$   
402 and  $\Phi_{id}$  are not independent estimates of  $\Phi$  because fitted on one another. This situation  
403 corresponds to the  $\Delta / \Delta$  fitting (fitting  $\Delta$  over  $\Delta$  corresponds to fitting  $\Phi_{MOD}$  over  $\Phi_{id}$  as the same  
404 model is used to interconvert  $\Phi$  and  $\Delta$ ). Note that the better fit between  $\Phi_{MOD}$  and  $\Phi_{id}$  not only is  
405 reached at expense of arising circularity, but also it distances  $J_{MOD}$  from  $J_{ATP}$ . When the distance  
406 between  $\Phi_{MOD}$  and  $\Phi_{id}$  is lowest (Figure 4 C), the distance between  $J_{MOD}$  and  $J_{ATP}$  is highest  
407 (Figure 3 A dotted lines). When the distance between  $\Phi_{MOD}$  and  $\Phi_{id}$  is highest (Figure 4 B), the  
408 distance between  $J_{MOD}$  and  $J_{ATP}$  is lowest (Figure 3 A solid lines).

#### 409 *Leakiness responses at decreasing PAR*

410 While the  $\Phi_{id}$  response for HL plants was expected, LL plants displayed a particular response  
411 that could not be simulated under conventional constraining of the C4 model. In HL plants,  
412 grown under PAR = 600  $\mu$ E m<sup>-2</sup> s<sup>-1</sup>,  $\Phi_{id}$  ranged from 0.17 to 0.66, in agreement with previous  
413 findings, and showed the conventional hyperbolic increase at decreasing PAR (Kromdijk *et al.*,  
414 2010, Ubierna *et al.*, 2011, Ubierna *et al.*, 2013, von Caemmerer & Furbank, 2003). However, in  
415 LL plants, grown under 100  $\mu$ E m<sup>-2</sup> s<sup>-1</sup>,  $\Phi_{id}$  was constant under decreasing PAR, a response that  
416 has not been shown before. In comparable studies, maize HL grown plants [ $500 \mu$ E m<sup>-2</sup> s<sup>-1</sup>  
417 (Ubierna *et al.*, 2013)] or maize plants grown under intermediate irradiance [ $250 \mu$ E m<sup>-2</sup> s<sup>-1</sup>  
418 (Kromdijk *et al.*, 2010)] showed a  $\Phi$  increase at low PAR. This increase was observed also in

419 other C4 species (Pengelly *et al.*, 2010, Tazoe *et al.*, 2008). In our experiment the gas exchange  
420 measurement routine may have contributed to showing the traits acquired during growth. The  
421 experiment included a strict 20 min short-term-acclimation after each change in PAR. During  
422 this time, LL plant metabolisms tuned and reach a status of low  $\Phi_{id}$ .

423 Interestingly, the  $\Phi_{id}$  trend observed in LL plants could not be simulated by the C4 model  
424 with the first fitting procedure, as the model described a hyperbolic increase of  $\Phi_{MOD}$  at  
425 decreasing PAR, similar to the  $\Phi_{id}$  response observed in HL plants. The hyperbolic increase is  
426 due to the effect constant  $x$  (the ATP partitioning between PEPC activity and C3 activity) and  
427  $R_{LIGHT}$ . In the C4 model, two contributions to CO<sub>2</sub> flux to BS are considered: i) the contribution  
428 of malate decarboxylation (equals PEPC activity at steady state); ii) the CO<sub>2</sub> respired in BS.  
429 When PAR decreases, while PEPC and Rubisco activities proportionally decrease, the BS  
430 respiration stays constant. In these conditions, BS-respired CO<sub>2</sub> is not fixed by the reduced  
431 Rubisco activity and is free to diffuse out of BS. As BS respiration progressively outweighs  $V_P$ ,  
432 the ratio of retrodiffusing CO<sub>2</sub> over PEP carboxylation rate ( $\Phi = L / V_P$ ) becomes progressively  
433 higher, hence the characteristic hyperbolic  $\Phi$  increase at limiting PAR. For these reasons the flat  
434  $\Phi_{id}$  response at decreasing PAR cannot be explained under the conventional model constraints:  
435 to explain the response we explored two scenarios involving unusual regulation of metabolism.

#### 436 *Acclimation scenarios*

437 By refitting the C4 model, we associated the flat  $\Phi_{id}$  pattern observed in LL plants with  
438 variable physiological traits. BS conductance to CO<sub>2</sub> ( $g_{BS}$ ) and the C4 / C3 ATP partitioning  
439 factor ( $x$ ) were chosen as their values were not derived from direct measurements and could be  
440 varied without changing the model assumptions or overriding data. Refitting differed from the  
441 fitting described above. Fitting assigned a value of  $g_{BS}$  to each individual plant, constant at all  
442 light intensities, and a value of  $x$ , constant for all plants in all conditions. In refitting, either  $x$  or  
443  $g_{BS}$  were varied between light intensities, while all other parameters were maintained as  
444 constants from the previous step. Refitting resulted in a tight match between  $\Phi_{MOD}$  and  $\Phi_{id}$  and,  
445 according to the parameter varied, described two alternative scenarios.

446 A first scenario explaining the flat  $\Phi_{id}$  pattern observed in LL plants involved variable  
447 partitioning between C4 and C3 activity ( $x$ ) as a function of light intensity. Under LL intensities  
448  $x$  was downregulated (Fig 5 A). This meant that the fraction of ATP consumed by PEPC over the  
449 total ATP consumed by assimilation became progressively lower. In other words, when PAR  
450 decreased, PEPC was downregulated more than the C3 activity and there was a shift from a  
451 PEPC-driven CCM to a respiration-driven CCM, effectively cutting the ATP cost of the CCM  
452 when light was limiting. This particular type of respiration-driven CCM resembles forms of  
453 CCM at the early stage of evolution of C4 photosynthesis (also known as C2 photosynthesis),  
454 when the biochemical exchange of acids between BS and M had not been optimized yet

455 (Griffiths *et al.*, 2013). As a consequence of the decreased CO<sub>2</sub> flux to BS,  $C_{BS}$  would decrease.  
456 To maintain a physiological assimilation rate (Fig 1 A) an increased activity of Rubisco would  
457 have to compensate for the lower  $C_{BS}$ . We could not quantify the differential Rubisco activity  
458 with the equations used here, because of the way the model is designed: Rubisco is assumed  
459 fully activated, saturated by RuBP and uniquely limited by  $J_{ATP}$ . The influence of differential  
460 relative Rubisco / PEPC activity on  $\Phi$  was shown in a modelling study, where the enzyme  
461 activation state was taken into account (Peisker & Henderson, 1992). A 10 % reduction in  
462 Rubisco activity relative to PEPC activity resulted in  $\Phi$  increasing by 14 %. A similar result was  
463 obtained experimentally in sugarcane where a 50 % higher relative Rubisco / PEPC activity  
464 measured in vitro corresponded to a 16 % lower  $\Phi$  estimated from isotopic discrimination of  
465 total leaf dry matter (Saliendra *et al.*, 1996).

466 The second scenario formulated to explain the flat  $\Phi_{id}$  pattern observed in LL plants, involved  
467 varying  $g_{BS}$  between light intensities. Under decreasing PAR, LL plants showed a differential  
468 capacity to retain CO<sub>2</sub> in BS. When, under limiting light, PEPC was downregulated, and CO<sub>2</sub>  
469 flux to BS was reduced, the CO<sub>2</sub> available in BS was trapped more effectively. In other words  
470 BS had the capacity to maintain high  $C_{BS}$  even under decreased PEPC activity. This relatively  
471 higher CO<sub>2</sub> concentration would maintain a physiological Rubisco carboxylation rate without  
472 any relative change in activity. Although counterintuitive, the idea of tuneable  $g_{BS}$  is supported  
473 by some theoretical considerations. Sowinsky and colleagues (2008) showed that the dimensions  
474 of plasmodesmata in maize are insufficient to account for a passive flow of solutes from BS to M  
475 at physiological rate, and they postulated the existence of active transport (mass flow or vesicle  
476 transport). If active transport is involved in metabolite trafficking, the cell could easily regulate  
477 the transport rate between M and BS, thus  $g_{BS}$ .

#### 478 *Wider implications*

479 The long-term and short-term acclimation to LL has implications at field level. In crop  
480 canopies leaves emerge fully exposed (equivalent to HL plants) and then undergo a low-light  
481 acclimation when progressively shaded by newly emerging leaves. We showed that maize leaves  
482 grown under HL did not short-term acclimate  $\Phi$  [in agreement with (Ubierna *et al.*, 2013)], nor  
483 did plants grown under intermediate light (Kromdijk *et al.*, 2010). However, plants grown under  
484 diffuse LL did display the capacity to short-term acclimate  $\Phi$  (flat  $\Phi$  response). We hypothesised  
485 two scenarios, both involving the capacity of optimising limiting ATP resources under low PAR.  
486 If plants were deploying similar strategies in the field, the impact of leakiness-dependent carbon  
487 losses at canopy scale may be much smaller than previously thought (Kromdijk *et al.*, 2008).

488 Future work will be oriented towards studying whether the ‘low leakiness state’ is also  
489 expressed under different light qualities and will investigate whether the ‘low leakiness at low

490 light state' can be induced in HL plants upon exposure to LL for a suitable acclimation period,  
491 thus mimicking the temporal transition that leaves undergo in the canopy.

## 492 **Conclusion**

493 The phenomenon of leakiness,  $\Phi$ , the amount of CO<sub>2</sub> diffusing out of the bundle sheath,  
494 expressed as relative to PEP carboxylation rate, was studied in maize by isotopic discrimination,  
495 gas exchange and photochemistry measurements. Respiration in the light and ATP production  
496 rate were measured directly. Data were interpreted using the established approach of fitting  $\Delta$  to  
497  $\Delta$  and using a novel approach of fitting  $J$  to  $J$  that removes the circularity of the  $\Delta / \Delta$  approach.

498 Plants grown in LL showed constant  $\Phi$  at decreasing light intensities, a response not reported  
499 in previous findings. This particular response was not predicted by the C4 model under common  
500 constraints but, by releasing the constraint of equal C4 / C3 energy partitioning ( $x$ ) or equal  
501 bundle sheath conductance between light intensities, it was possible to formulate hypotheses to  
502 describe the two different acclimation strategies. HL plants operated efficiently at HL but  
503 maintained a high PEPC activity at low light, resulting in high CO<sub>2</sub> overcycling. At limiting light  
504 intensities LL plants downregulated PEPC more than proportionally to the C3 activity and there  
505 was a shift from a PEPC-driven CCM to a respiration-driven CCM, effectively cutting the ATP  
506 cost of the CCM when light was limiting. Physiological assimilation rates were maintained either  
507 by increasing Rubisco activity or by tuning  $g_{BS}$ , effectively trapping the CO<sub>2</sub> resulting from  
508 decarboxylation of malate and pyruvate. In both cases the plant could optimise scarce ATP  
509 resources. The actual impact of leakiness on canopy net photosynthetic uptake may need to be  
510 revised in light of this surprising acclimation plasticity.

## 511 **Acknowledgments**

512 We are deeply grateful to Asaph Cousins, Johannes Kromdijk, Jeremy Harbinson and Xinyou  
513 Yin for the kind hospitality in their labs and the fruitful and stimulating exchange of ideas, to  
514 Johannes Kromdijk for contribution to the manuscript and review, Madeline Mitchell and Jessica  
515 Royles for review, to Davide Gusberty for seeds, to Bayer Crop Science and Syngenta for the  
516 material provided. Funding: EU FP7 Marie curie ITN Harvest, grant n° 238017.

517 The Authors have no conflict of interest.

## References

- Baker N.R. & Long S.P. (1988) *Photosynthesis and temperature, with particular reference to effects on quantum yield*. Paper presented at the Plants and temperature: Society for Experimental Biology Symposium No XXXXII.
- Barbour M.M., McDowell N.G., Tcherkez G., Bickford C.P. & Hanson D.T. (2007) A new measurement technique reveals rapid post-illumination changes in the carbon isotope composition of leaf-respired CO<sub>2</sub>. *Plant Cell and Environment*, **30**, 469-482.
- Covshoff S. & Hibberd J.M. (2012) Integrating C-4 photosynthesis into C-3 crops to increase yield potential. *Current Opinion in Biotechnology*, **23**, 209-214.
- Craig H. (1953) The Geochemistry of the Stable Carbon Isotopes. *Geochimica Et Cosmochimica Acta*, **3**, 53-92.
- D'Ambrosio N., Arena C. & Virzo de Santo A. (2003) Different Relationship Between Electron Transport and CO<sub>2</sub> Assimilation in two Zea mays cultivars as Influenced by Increasing Irradiance. *Photosynthetica*, **41**, 489-495.
- Dougherty R.L., Bradford J.A., Coyne P.I. & Sims P.L. (1994) Applying an empirical model of stomatal conductance to three C<sub>4</sub> grasses. *Agricultural and Forest Meteorology*, **67**, 269-290.
- Driscoll S.P., Prins A., Olmos E., Kunert K.J. & Foyer C.H. (2006) Specification of adaxial and abaxial stomata, epidermal structure and photosynthesis to CO<sub>2</sub> enrichment in maize leaves. *Journal of Experimental Botany*, **57**, 381-390.
- Edwards G.E. & Baker N.R. (1993) Can CO<sub>2</sub> assimilation in maize leaves be predicted accurately from chlorophyll fluorescence analysis. *Photosynthesis Research*, **37**, 89-102.
- Evans J.R., Sharkey T.D., Berry J.A. & Farquhar G.D. (1986) Carbon Isotope Discrimination Measured Concurrently with Gas-Exchange to Investigate CO<sub>2</sub> Diffusion in Leaves of Higher-Plants. *Australian Journal of Plant Physiology*, **13**, 281-292.
- FAO (2012) Fao Statistical division web page, Rome.
- Farquhar G.D. (1983) On the Nature of Carbon Isotope Discrimination in C<sub>4</sub> Species. *Australian Journal of Plant Physiology*, **10**, 205-226.
- Farquhar G.D. & Cernusak L.A. (2012) Ternary effects on the gas exchange of isotopologues of carbon dioxide. *Plant Cell and Environment*, **35**, 1221-1231.
- Farquhar G.D., von Caemmerer S. & Berry J.A. (1980) A biochemical-model of photosynthetic CO<sub>2</sub> assimilation in leaves of C<sub>3</sub> species. *Planta*, **149**, 78-90.
- Flexas J., Diaz-Espejo A., Berry J.A., Cifre J., Galmes J., Kaidenhoff R., Medrano H. & Ribas-Carbo M. (2007) Analysis of leakage in IRGA's leaf chambers of open gas exchange systems: quantification and its effects in photosynthesis parameterization. *Journal of Experimental Botany*, **58**, 1533-1543.
- Furbank R., Jenkins C. & Hatch M. (1990) C<sub>4</sub> Photosynthesis: Quantum Requirement, C<sub>4</sub> and Overcycling and Q-Cycle Involvement. *Functional Plant Biology*, **17**, 1-7.
- Gandin A. & Cousins A.B. (2012) *The contribution of respiratory fractionation to leaf CO<sub>2</sub> isotope exchange in the C<sub>3</sub> plant Nicotina tabacum*. Paper presented at the 21st Western Photosynthesis Conference, Asilomar Conference Grounds Pacific Grove, California, USA.
- Genty B., Briantais J.M. & Baker N.R. (1989) The relationship between the quantum yield of photosynthetic electron-transport and quenching of chlorophyll fluorescence. *Biochimica Et Biophysica Acta*, **990**, 87-92.
- Ghashghaie J., Duranceau M., Badeck F.W., Cornic G., Adeline M.T. & Deleens E. (2001)  $\delta^{13}\text{C}$  of CO<sub>2</sub> respired in the dark in relation to  $\delta^{13}\text{C}$  of leaf metabolites: comparison between Nicotiana sylvestris and Helianthus annuus under drought. *Plant Cell and Environment*, **24**, 505-515.
- Gillon J.S. & Griffiths H. (1997) The influence of (photo)respiration on carbon isotope discrimination in plants. *Plant Cell and Environment*, **20**, 1217-1230.
- Griffiths H., Broadmeadow M.S.J., Borland A.M. & Hetherington C.S. (1990) Short-Term Changes in Carbon-Isotope Discrimination Identify Transitions between C<sub>3</sub> and C<sub>4</sub> Carboxylation during Crassulacean Acid Metabolism. *Planta*, **181**, 604-610.
- Griffiths H., Weller G., Toy L.F.M. & Dennis R.J. (2013) You're so vein: bundle sheath physiology, phylogeny and evolution in C<sub>3</sub> and C<sub>4</sub> plants. *Plant, Cell & Environment*, **36**, 249-261.
- Henderson S.A., Von Caemmerer S. & Farquhar G.D. (1992) Short-Term Measurements of Carbon Isotope Discrimination in Several C<sub>4</sub> Species. *Australian Journal of Plant Physiology*, **19**, 263-285.
- Hymus G.J., Maseyk K., Valentini R. & Yakir D. (2005) Large daily variation in C-13-enrichment of leaf-respired CO<sub>2</sub> in two Quercus forest canopies. *New Phytologist*, **167**, 377-384.
- Igamberdiev A.U., Mikkelsen T.N., Ambus P., Bauwe H., Lea P.J. & Gardestrom P. (2004) Photorespiration contributes to stomatal regulation and carbon isotope fractionation: a study with barley, potato and Arabidopsis plants deficient in glycine decarboxylase. *Photosynthesis Research*, **81**, 139-152.
- Kajala K., Covshoff S., Karki S., Woodfield H., Tolley B.J., Dionora M.J.A., Mogul R.T., Mabilangan A.E., Danila F.R., Hibberd J.M. & Quick W.P. (2011) Strategies for engineering a two-celled C<sub>4</sub> photosynthetic pathway into rice. *Journal of Experimental Botany*, **62**, 3001-3010.
- Krall J.P. & Edwards G.E. (1990) Quantum yields of photosystem-ii electron-transport and carbon-dioxide fixation in c<sub>4</sub>-plants. *Australian Journal of Plant Physiology*, **17**, 579-588.
- Kromdijk J., Griffiths H. & Schepers H.E. (2010) Can the progressive increase of C<sub>4</sub> bundle sheath leakiness at low PFD be explained by incomplete suppression of photorespiration? *Plant Cell and Environment*, **33**, 1935-1948.
- Kromdijk J., Schepers H.E., Albanito F., Fitton N., Carroll F., Jones M.B., Finnan J., Lanigan G.J. & Griffiths H. (2008) Bundle Sheath Leakiness and Light Limitation during C<sub>4</sub> Leaf and Canopy CO<sub>2</sub> Uptake. *Plant Physiology*, **148**, 2144-2155.
- Lanigan G.J., Betson N., Griffiths H. & Seibt U. (2008) Carbon Isotope Fractionation during Photorespiration and Carboxylation in Senecio. *Plant Physiology*, **148**, 2013-2020.
- Long S.P. & Bernacchi C.J. (2003) Gas exchange measurements, what can they tell us about the underlying limitations to photosynthesis? Procedures and sources of error. *Journal of Experimental Botany*, **54**, 2393-2401.
- Mook W.G., Bommerso.Jc & Staverma.Wh (1974) Carbon Isotope Fractionation between Dissolved Bicarbonate and Gaseous Carbon-Dioxide. *Earth and Planetary Science Letters*, **22**, 169-176.
- O'Leary M.H. (1984) Measurement of the isotope fractionation associated with diffusion of carbon dioxide in aqueous solution. *The Journal of Physical Chemistry*, **88**, 823-825.
- Oberhuber W., Dai Z.Y. & Edwards G.E. (1993) Light dependence of quantum yields of photosystem-ii and CO<sub>2</sub> fixation in C<sub>3</sub> and C<sub>4</sub> plants. *Photosynthesis Research*, **35**, 265-274.
- Osborne C.P. & Sack L. (2012) Evolution of C<sub>4</sub> plants: a new hypothesis for an interaction of CO<sub>2</sub> and water relations mediated by plant hydraulics. *Philosophical Transactions of the Royal Society B-Biological Sciences*, **367**, 583-600.
- Pearcy R.W. & Ehleringer J. (1984) Comparative ecophysiology of C<sub>3</sub> and C<sub>4</sub> plants. *Plant, Cell & Environment*, **7**, 1-13.
- Peisker M. & Henderson S.A. (1992) Carbon - terrestrial c<sub>4</sub> plants. *Plant Cell and Environment*, **15**, 987-1004.
- Pengelly J.J.L., Sirault X.R.R., Tazoe Y., Evans J.R., Furbank R.T. & von Caemmerer S. (2010) Growth of the C<sub>4</sub> dicot Flaveria bidentis: photosynthetic acclimation to low light through shifts in leaf anatomy and biochemistry. *Journal of Experimental Botany*, **61**, 4109-4122.
- Pons T.L., Flexas J., von Caemmerer S., Evans J.R., Genty B., Ribas-Carbo M. & Brugnoli E. (2009) Estimating mesophyll conductance to CO<sub>2</sub>: methodology, potential errors, and recommendations. *Journal of Experimental Botany*, **60**, 2217-2234.
- Prioul J.L. & Chartier P. (1977) Partitioning of Transfer and Carboxylation Components of Intracellular Resistance to Photosynthetic CO<sub>2</sub> Fixation: A Critical Analysis of the Methods Used. *Annals of Botany*, **41**, 789-800.
- Roeske C.A. & O'Leary M.H. (1984) Carbon Isotope Effects on the Enzyme-Catalyzed Carboxylation of Ribulose Bisphosphate. *Biochemistry*, **23**, 6275-6284.

- Saliendra N.Z., Meinzer F.C., Perry M. & Thom M. (1996) Associations between partitioning of carboxylase activity and bundle sheath leakiness to CO<sub>2</sub>, carbon isotope discrimination, photosynthesis, and growth in sugarcane. *Journal of Experimental Botany*, **47**, 907-914.
- Sheehy J.E., ed (2008) *Charting New Pathways to C4 Rice*. World Scientific Publishing, Singapore.
- Sowinski P., Szczepanik J. & Minchin P.E.H. (2008) On the mechanism of C4 photosynthesis intermediate exchange between Kranz mesophyll and bundle sheath cells in grasses. *Journal of Experimental Botany*, **59**, 1137-1147.
- Sun W.E.I., Ubierna N., Ma J.-Y. & Cousins A.B. (2012) The influence of light quality on C4 photosynthesis under steady-state conditions in *Zea mays* and *Miscanthus × giganteus*: changes in rates of photosynthesis but not the efficiency of the CO<sub>2</sub> concentrating mechanism. *Plant, Cell & Environment*, **35**, 982-993.
- Tazoe Y., Hanba Y.T., Furumoto T., Noguchi K. & Terashima I. (2008) Relationships between quantum yield for CO<sub>2</sub> assimilation, activity of key enzymes and CO<sub>2</sub> leakiness in *Amaranthus cruentus*, a C4 dicot, grown in high or low light. *Plant and Cell Physiology*, **49**, 19-29.
- Tcherkez G., Bligny R., Gout E., Mahé A., Hodges M. & Cornic G. (2008) Respiratory metabolism of illuminated leaves depends on CO<sub>2</sub> and O<sub>2</sub> conditions. *Proceedings of the National Academy of Sciences*, **105**, 797-802.
- Ubierna N., Sun W. & Cousins A.B. (2011) The efficiency of C4 photosynthesis under low light conditions: assumptions and calculations with CO<sub>2</sub> isotope discrimination. *Journal of Experimental Botany*, **62**, 3119-3134.
- Ubierna N., Sun W., Kramer D.M. & Cousins A.B. (2013) The Efficiency Of C4 Photosynthesis Under Low Light Conditions In *Zea Mays*, *Miscanthus X Giganteus* And *Flaveria Bidentis*. *Plant, Cell & Environment*, **36**, 365-381.
- Vogel J.C. (1980) *Fractionation of the carbon isotopes during photosynthesis*. Springer, Berlin and New York.
- Vogel J.C., Grootes P.M. & Mook W.G. (1970) Isotopic Fractionation between Gaseous and Dissolved Carbon Dioxide. *Zeitschrift Fur Physik*, **230**, 225-238.
- von Caemmerer S. (2000) *Biochemical models of leaf Photosynthesis*. Csiro.
- von Caemmerer S. & Farquhar G.D. (1981) Some Relationships between the Biochemistry of Photosynthesis and the Gas-Exchange of Leaves. *Planta*, **153**, 376-387.
- von Caemmerer S. & Furbank R.T. (2003) The C4 pathway: an efficient CO<sub>2</sub> pump. *Photosynthesis Research*, **77**, 191-207.
- Wingate L., Seibt U., Moncrieff J.B., Jarvis P.G. & Lloyd J. (2007) Variations in <sup>13</sup>C discrimination during CO<sub>2</sub> exchange by *Picea sitchensis* branches in the field. *Plant Cell and Environment*, **30**, 600-616.
- Yin X. & Struik P.C. (2009) C3 and C4 photosynthesis models: An overview from the perspective of crop modelling. *Njas-Wageningen Journal of Life Sciences*, **57**, 27-38.
- Yin X., Sun Z., Struik P.C. & Gu J. (2011a) Evaluating a new method to estimate the rate of leaf respiration in the light by analysis of combined gas exchange and chlorophyll fluorescence measurements. *Journal of Experimental Botany*, **62**, 3489-3499.
- Yin X.Y., Sun Z.P., Struik P.C., Van der Putten P.E.L., Van Ieperen W. & Harbinson J. (2011b) Using a biochemical C4 photosynthesis model and combined gas exchange and chlorophyll fluorescence measurements to estimate bundle-sheath conductance of maize leaves differing in age and nitrogen content. *Plant Cell and Environment*, **34**, 2183-2199.

## Tables.

**Table 1.** Abbreviations, definitions and units for variables and acronyms described in the text.

Symbol	Definition	Values/Units
$\delta$	Isotopic composition relative to Pee dee belemnite	‰
$a$	$^{13}\text{C}$ fractionation due to diffusion of $\text{CO}_2$ in air. Because of vigorous ventilation we neglected the fractionation of the boundary layer (Kromdijk <i>et al.</i> , 2010).	4.4 ‰ (Craig, 1953)
$A$	Net assimilation	$\mu\text{mol m}^{-2} \text{s}^{-1}$
$a_d$	$^{13}\text{C}$ fractionation due to diffusion of $\text{CO}_2$ in water	0.7 ‰ (O'Leary, 1984)
ATP	Adenosine triphosphate	
$b_3$	$^{13}\text{C}$ fractionation during carboxylation by Rubisco including respiration and photorespiration fractionation $b_3 = b'_3 - \frac{e \cdot R_{\text{LIGHT}} + f \cdot V_o}{V_c}$ (Farquhar, 1983).	‰
$b_3'$	$^{13}\text{C}$ fractionation during carboxylation by Rubisco	30 ‰ (Roeske & O'Leary, 1984)
$b_4$	Net fractionation by $\text{CO}_2$ dissolution, hydration and PEPC carboxylation including respiratory fractionation $b_4 = b'_4 - \frac{e' \cdot R_M}{V_p}$ (Farquhar, 1983, Henderson <i>et al.</i> , 1992).	‰
$b_4'$	Net fractionation by $\text{CO}_2$ dissolution, hydration and PEPC carboxylation.	-5.7 ‰ at 25 °C but variable with temperature (Farquhar, 1983, Henderson <i>et al.</i> , 1992, Kromdijk <i>et al.</i> , 2010).
BS	Bundle sheath	
$C_a$	$\text{CO}_2$ concentration in the cuvette as measured by IRGA	$\mu\text{mol mol}^{-1}$
$C_{BS}$	$\text{CO}_2$ concentration in the bundle sheath	$\mu\text{mol mol}^{-1}$
$C_i$	$\text{CO}_2$ concentration in the intercellular spaces as calculated by the IRGA (Li-cor manual Eqn 1-18).	$\mu\text{mol mol}^{-1}$
$C_M$	$\text{CO}_2$ concentration in the mesophyll Eqn 8	$\mu\text{mol mol}^{-1}$
$e$	$^{13}\text{C}$ fractionation during decarboxylation	0 ‰ to -10 ‰ (Barbour <i>et al.</i> , 2007, Ghashghaie <i>et al.</i> , 2001, Gillon & Griffiths, 1997, Hymus <i>et al.</i> , 2005, Igamberdiev <i>et al.</i> , 2004, Sun <i>et al.</i> , 2012), -6 ‰ in this study (Kromdijk <i>et al.</i> , 2010).
$e'$	$^{13}\text{C}$ fractionation during decarboxylation, including the correction for measurement artefacts: $e' = e + \delta^{13}\text{C}_{\text{measurements}} - \delta^{13}\text{C}_{\text{growth chamber}}$ In this study $\delta^{13}\text{C}_{\text{measurements}} = -9.46$ ‰; $\delta^{13}\text{C}_{\text{growth chamber}} = -8$ ‰ (Wingate <i>et al.</i> , 2007)	‰
$e_s$	$^{13}\text{C}$ fractionation during internal $\text{CO}_2$ dissolution	1.1 ‰ (Mook <i>et al.</i> , 1974, Vogel, 1980, Vogel <i>et al.</i> , 1970).
$f$	$^{13}\text{C}$ fractionation during photorespiration.	-11.6 ‰ (Lanigan <i>et al.</i> , 2008).
$F_s$	Steady state fluorescence signal	Volts, arbitrary
$F_m$	Maximum fluorescence signal of dark adapted leaves	Volts, arbitrary
$F_m'$	Saturating pulse induced F signal during steady state photosynthesis	Volts, arbitrary
GA	Gross assimilation $GA = A + R_{\text{LIGHT}}$	$\mu\text{mol m}^{-2} \text{s}^{-1}$
$g_{BS}$	Bundle sheath conductance to $\text{CO}_2$ , calculated by curve fitting	$\text{mol m}^{-2} \text{s}^{-1}$
$g_M$	Mesophyll conductance to $\text{CO}_2$	$1 \text{ mol m}^{-2} \text{s}^{-1} \text{ bar}^{-1}$ (Kromdijk <i>et al.</i> , 2010)
$g_s$	Stomata conductance to $\text{CO}_2$	$\text{mol m}^{-2} \text{s}^{-1}$
HL	High light	
IRGA	Infra red gas analyzer	
$J_{MOD}$	Modelled ATP production rate Eqn 9	$\mu\text{E m}^{-2} \text{s}^{-1}$
$J_{ATP}$	ATP production rate	$\mu\text{mol m}^{-2} \text{s}^{-1}$
$J_{ATP \text{ Low}}$	ATP production rate at low $\text{O}_2$ and high $\text{CO}_2$ , Eqn 1	$\mu\text{mol m}^{-2} \text{s}^{-1}$
$\text{O}_2$		
L	Rate of $\text{CO}_2$ Leakage from BS to M Eqn 6	$\mu\text{mol m}^{-2} \text{s}^{-1}$
LL	Low light	
M	Mesophyll	
$O_M$	$\text{O}_2$ mol fraction in the mesophyll cells (in air at equilibrium)	210000 $\mu\text{mol mol}^{-1}$
$O_{BS}$	$\text{O}_2$ mol fraction in the bundle sheath cells (in air at equilibrium) $O_{BS} = O_M + \frac{\alpha A}{0.047 g_{BS}}$ (von Caemmerer, 2000)	$\mu\text{mol mol}^{-1}$
PAR	Photosynthetically active radiation	$\mu\text{E m}^{-2} \text{s}^{-1}$
PEP	Phosphoenolpyruvate	
PEPC	Phosphoenolpyruvate carboxylase	
$R_{\text{LIGHT}}$	Total non photorespiratory $\text{CO}_2$ production in the light	$\mu\text{mol m}^{-2} \text{s}^{-1}$
$R_M$	Mesophyll non photorespiratory $\text{CO}_2$ production in the light $R_M = 0.5 R_{\text{LIGHT}}$ (Kromdijk <i>et al.</i> , 2010, Ubierna <i>et al.</i> , 2011, von Caemmerer, 2000)	$\mu\text{mol m}^{-2} \text{s}^{-1}$
Rubisco	Ribulose biphosphate carboxylase oxygenase	
$s$	Fractionation during leakage of $\text{CO}_2$ out of the bundle sheath cells	1.8 ‰ (Henderson <i>et al.</i> , 1992).
$s'$	Lumped conversion efficiency. Includes leaf absorptance, the partitioning of light to photosystem II and the conversion of energy into ATP (Yin & Struik, 2009, Yin <i>et al.</i> , 2011b)	Dimensionless
$t$	Ternary effects $t = \frac{(1+a)E}{2000 g_{ac}}$ where $E / \text{mmol m}^{-2} \text{s}^{-1}$ is the transpiration rate (calculated by the IRGA software, parameter Trmmol), $g_{ac} / \text{mol m}^{-2} \text{s}^{-1}$ is the conductance to diffusion of $\text{CO}_2$ in air (calculated by the IRGA software, parameter CndCO2), $a$ is the isotopic fractionation during diffusion in air.	‰ (Farquhar & Cernusak, 2012)<
$V_c$	Rubisco carboxylation rate $V_c = \frac{(A+R_{\text{LIGHT}})}{1 - \frac{C_{BS}}{C_a}}$ (Ubierna <i>et al.</i> , 2011)	$\mu\text{mol m}^{-2} \text{s}^{-1}$
$V_o$	Rubisco oxygenation rate $V_o = \frac{V_c - A - R_{\text{LIGHT}}}{0.5}$ (Ubierna <i>et al.</i> , 2011)	$\mu\text{mol m}^{-2} \text{s}^{-1}$
$V_p$	PEP carboxylation rate Eqn 7	$\mu\text{mol m}^{-2} \text{s}^{-1}$
$x$	Partitioning factor of $J_{ATP}$ between C4 activity $V_p$ (PEP regeneration and PEP carboxylation, Eqn 7) and C3 activity $V_c + V_o$ (reductive pentose phosphate pathway and photorespiratory cycle)	0.4 (Kromdijk <i>et al.</i> , 2010, Ubierna <i>et al.</i> , 2011, Ubierna <i>et al.</i> , 2013, von Caemmerer, 2000)
$\alpha$	Fraction of PSII active in BS cells	0.15 (Edwards & Baker, 1993, Kromdijk <i>et al.</i> , 2010, von Caemmerer, 2000).
$\gamma^*$	Half of the reciprocal of the Rubisco specificity	0.000193 (von Caemmerer, 2000).
$\Delta$	Carbon isotope discrimination against $^{13}\text{C}$	‰
$\Delta_{OBS}$	Observed carbon isotope discrimination against $^{13}\text{C}$ , Eqn 16 supporting text 1	‰
$\Phi$	Leakiness $\Phi = L/V_p$	dimensionless
$\Phi_d$	Leakiness estimated with the isotope method including respiratory and photorespiratory fractionation and calculating $C_{BS}$ Eqn 3 (Ubierna <i>et al.</i> , 2011)	dimensionless
$\Phi_{MOD}$	Leakiness estimated with the C4 light limited photosynthesis equations Eqn 11	dimensionless
$Y(II)$	Yield of photosystem II $Y(II) = \frac{F_m - F_s}{F_m}$ (Genty <i>et al.</i> , 1989)	dimensionless

**Table 2.** Response of HL plants and LL plants to different O<sub>2</sub> concentrations. Assimilation at 50 μE m<sup>-2</sup> s<sup>-1</sup> (A<sub>50</sub>) is shown to exemplify limiting light conditions. The compensation point  $\Gamma$  was determined fitting a quadratic equation with the use of dedicated software (Photosyn assistant 1.2, Dundee Scientific, Dundee, UK) (Dougherty *et al.*, 1994, Prioul & Chartier, 1977). Respiration in the light  $R_{LIGHT}$  was determined by linear regression of  $A$  against PAR· $Y(II)$  / 3 (see supporting Text 1).  $s'$  was the slope of the linear regression of  $A$  against PAR· $Y(II)$  / 3 and represented the lumped conversion efficiency of PAR into ATP. Values were not significantly different in a t-test for P < 0.05. n = 7

	Unit	21 % O <sub>2</sub>		2 % O <sub>2</sub>	
		LL	HL	LL	HL
A <sub>50</sub>	μmol m <sup>-2</sup> s <sup>-1</sup>	2.29 ± 0.0096	1.83 ± 0.022	2.69 ± 0.11	2.10 ± 0.18
$\Gamma$	μE m <sup>-2</sup> s <sup>-1</sup>	8.35 ± 0.12	17.0 ± 0.18	3.83 ± 1.4	12.3 ± 2.8
$R_{LIGHT}$	μmol m <sup>-2</sup> s <sup>-1</sup>	0.520 ± 0.017	1.00 ± 0.069	0.291 ± 0.036	0.924 ± 0.099
$s'$	1	0.224 ± 0.0019	0.225 ± 0.0062	0.231 ± 0.0044	0.248 ± 0.0094

**Table 3** Bundle sheath conductance estimated by curve fitting.  $J / J$  fitted a modelled ATP production ratio ( $J_{MOD}$ ), on a measured  $J_{ATP}$  (determined with the chlorophyll fluorescence – low O<sub>2</sub> method).  $\Delta / \Delta$  fitted a modelled isotopic discrimination  $\Delta_{MOD}$ , to the measured isotopic discrimination  $\Delta_{OBS}$ . Different letters were deemed significant for P < 0.05 in a Tukey multiple comparison test (Genstat). Average values ± S.D. LL n = 4; HL n = 3.

Fitting approach	Unit	$g_{BS}$	
		LL	HL
$J / J$	mol m <sup>-2</sup> s <sup>-1</sup>	8.20·10 <sup>-4</sup> ± 1.4·10 <sup>-4</sup> a	10.3·10 <sup>-4</sup> ± 1.8·10 <sup>-4</sup> a
$\Delta / \Delta$	mol m <sup>-2</sup> s <sup>-1</sup>	12.7·10 <sup>-4</sup> ± 1.5·10 <sup>-4</sup> a	46.4·10 <sup>-4</sup> ± 8.5·10 <sup>-4</sup> b

## Figures

**Figure 1.** Gas exchange responses of HL and LL plants. LL plants (triangles) and HL plants (squares) under low  $O_2$  (open symbols) or ambient air (filled symbols) were exposed to decreasing light intensity. **(A)**: net assimilation,  $A$ . The curves were fitted in order to calculate the compensation point with the use of dedicated software (Photosyn assistant 1.2, Dundee Scientific, Dundee, UK) (Dougherty *et al.*, 1994, Prioul & Chartier, 1977). The inset shows a magnification in the vicinity of the compensation point. **(B)**:  $C_i / C_a$ . **(C)**: stomatal conductance,  $g_s$ . Error bars represent standard error. HL n = 3; LL n = 4.

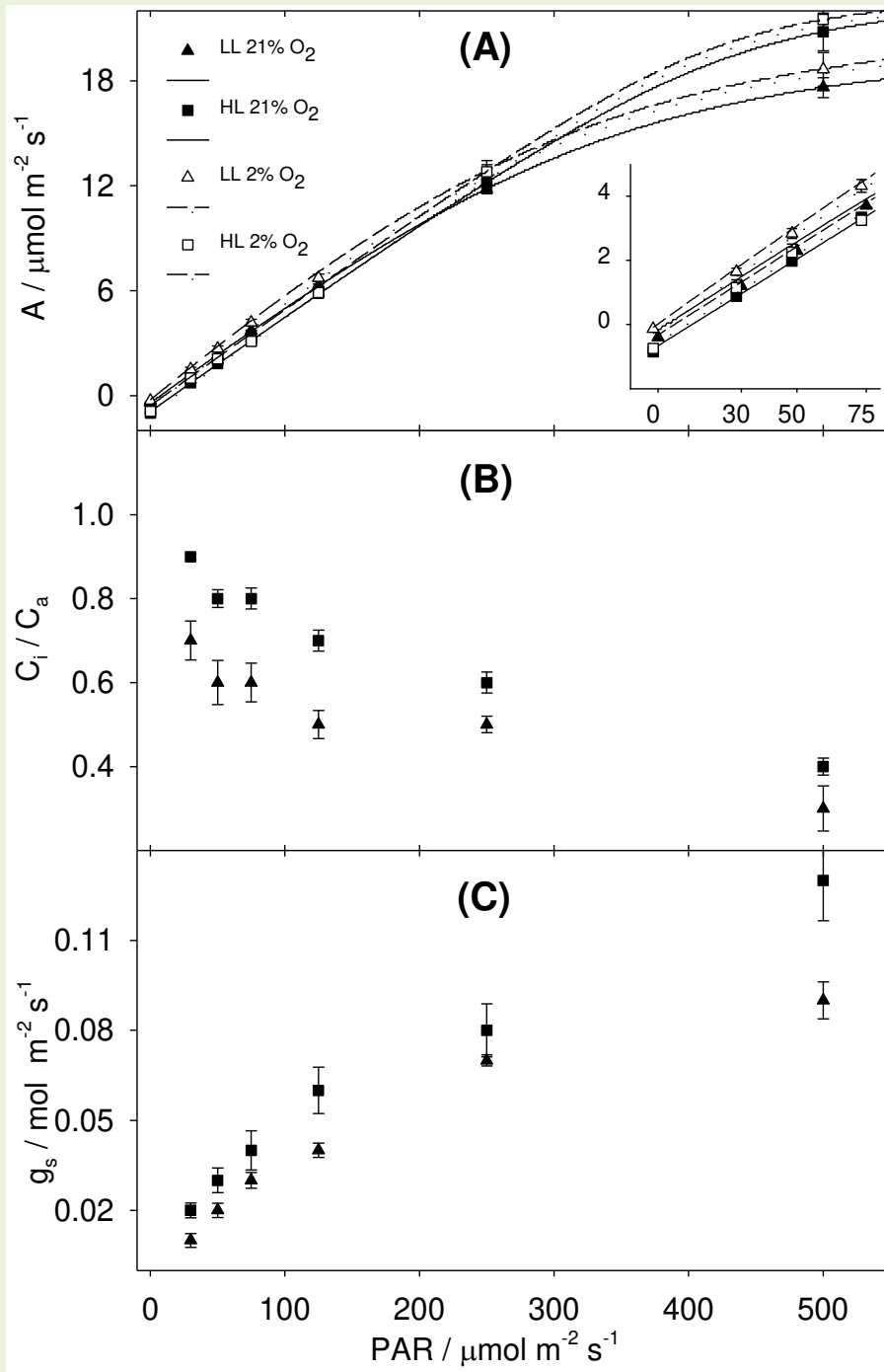


**Figure 2.** Yield of photosystem II,  $Y(II)$  at decreasing light intensity. Response of  $Y(II)$  of HL plants (A) and LL plants (B) measured in low  $O_2$  (open symbols) or ambient air (filled symbols) to decreasing light intensities. Error bars represent standard error.  $n = 4$ .

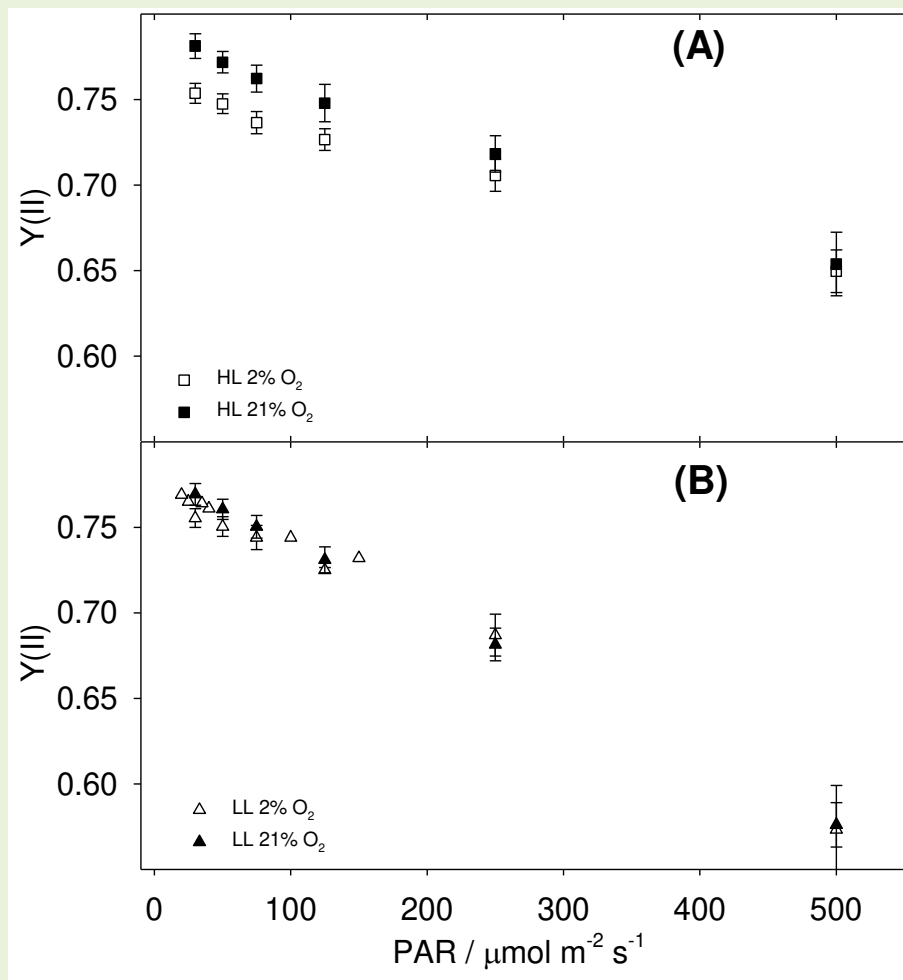


**Figure 3.** Datasets and model fitting.

- 1) Total ATP production rate,  $J_{ATP}$ , and isotopic discrimination during photosynthesis  $\Delta_{OBS}$ . Symbols in panel (A) show  $J_{ATP}$  for LL plants (triangles) and HL plants (squares). Symbols in panel (B) show  $\Delta_{OBS}$  for LL plants (triangles) and for HL plants (squares).
- 2) Model fitting with J / J and  $\Delta$  /  $\Delta$  approaches. In order to estimate  $g_{BS}$ , the C4 photosynthesis model (lines) was fitted to the two different datasets alternatively. In the J / J approach the C4 model (solid lines) was expressed as  $J_{MOD}$  and fitted to  $J_{ATP}$  measured on LL plants (Panel (A), thin solid line) and to  $J_{ATP}$  measured on HL plants [Panel (A), thick solid line]. In the  $\Delta$  /  $\Delta$  approach the C4 model (dotted lines) was expressed as  $\Delta_{MOD}$  and fitted to  $\Delta_{OBS}$  measured on LL plants [Panel (B), thin dotted line] and on  $\Delta_{OBS}$  measured on HL plants (Panel (B), thick dotted line).
- 3) Note the trade-off between fitting approaches. As the C4 model is the same, by fitting  $J_{MOD}$  to  $J_{ATP}$ ,  $\Delta_{MOD}$  is distanced from  $\Delta_{OBS}$  [see solid lines in panel (B)]. Similarly, by fitting  $\Delta_{MOD}$  to  $\Delta_{OBS}$ ,  $J_{MOD}$  is distanced from  $J_{ATP}$  [see dotted lines in panel (A)]. Error bars represent standard error. HL n = 3; LL n = 4.

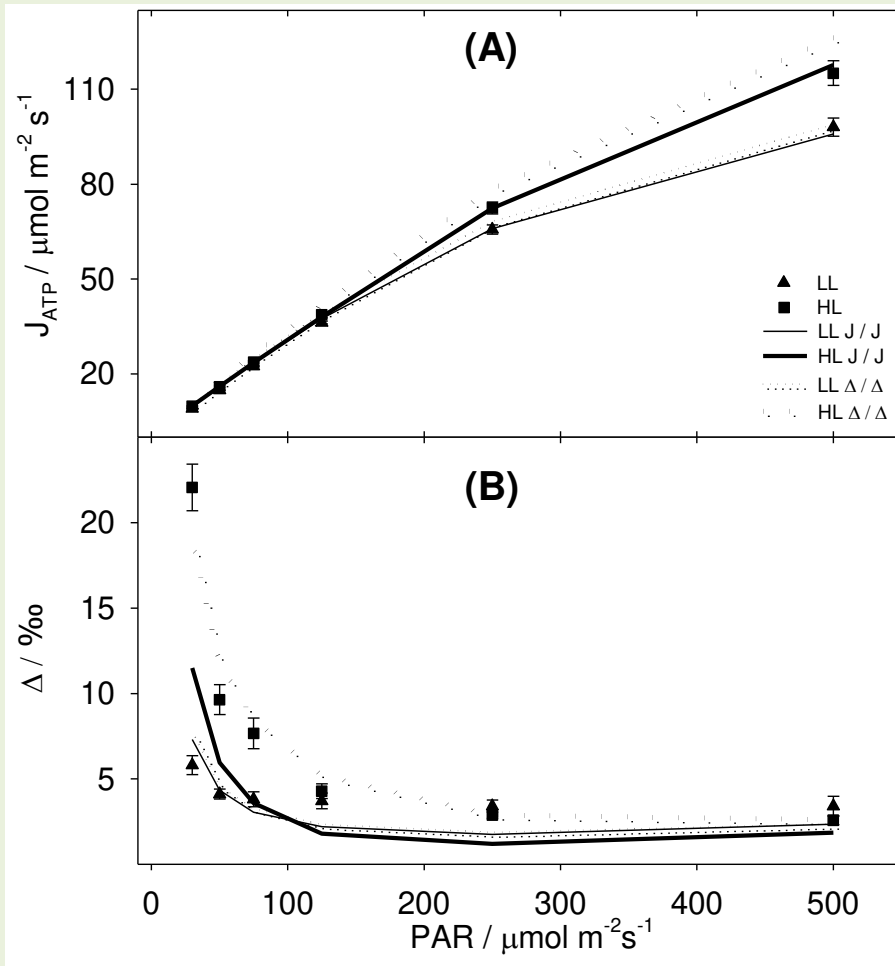


**Figure 4.** Output of the C4 model and the isotopic discrimination model.

(A): response of  $C_{BS}$ , calculated either with  $J / J$  approach (solid lines), or with the  $\Delta / \Delta$  approach (dotted lines), of LL plants (thin lines) and HL plants (thick lines) to decreasing light intensities.

(B):  $J / J$  approach. Symbols represent leakiness based on isotopic discrimination data  $\Phi_{id}$  (Eqn 3) for LL plants (triangles) and for HL plants (squares); lines represent modelled leakiness  $\Phi_{MOD}$  (Eqn 11) for LL plants (thin solid line) and for HL plants (thick solid line).

(C):  $\Delta / \Delta$  approach. Symbols represent leakiness based on isotopic discrimination data  $\Phi_{id}$  (Eqn 3) for LL plants (triangles) and for HL plants (squares); lines represent modelled leakiness  $\Phi_{MOD}$  (Eqn 11) for LL plants (thin dotted lines) and for HL plants (thick dotted line).

Error bars represent standard error. HL n = 3; LL n = 4.

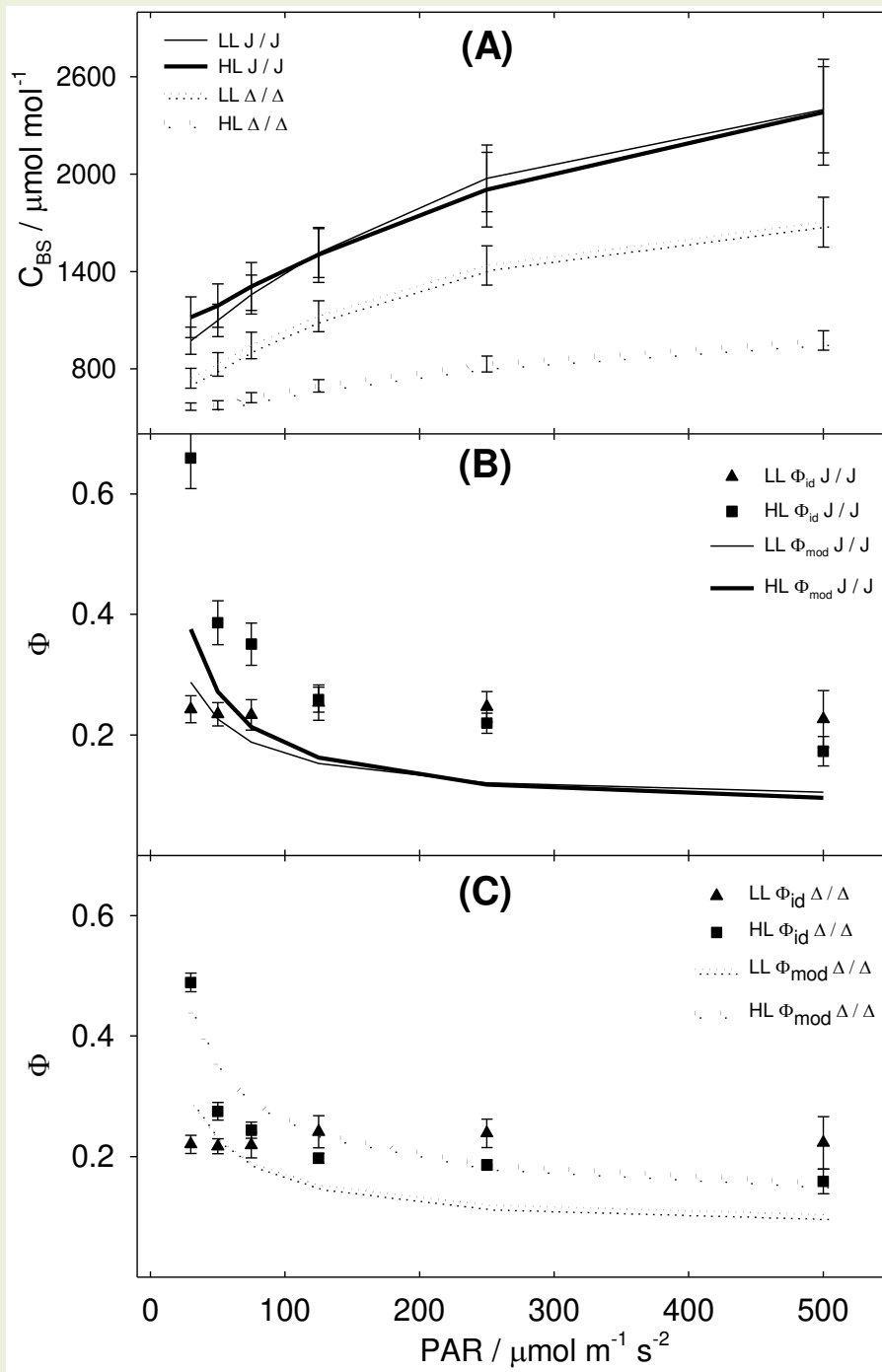


**Figure 5.** Model refitting. In panel (A)  $\Phi_{MOD}$  was fitted to  $\Phi_{id}$  varying  $x$  between light intensities.  $x$  is the factor partitioning  $J_{ATP}$  between C4 activity (PEPC carboxylation) and the C3 activity (RPP cycle + glyoxylate recycling). The line displayed is an inverse quadratic regression fitted to LL data. In panel (B)  $\Phi_{MOD}$  was fitted to  $\Phi_{id}$  varying bundle sheath conductance  $g_{BS}$  between light intensities. The line displayed is a quadratic regression fitted to LL data. All the other parameters were unvaried from the previous fitting step. Error bars represent standard error. HL n = 3; LL n = 4.

